

A Rapid and Robust Diagnostic for Liver Fibrosis Using a Multichannel Polymer Sensor Array

William J. Peveler, Ryan F. Landis, Mahdieh Yazdani, James W. Day, Raakesh Modi, Claire J. Carmalt, William M. Rosenberg,* and Vincent M. Rotello*

Liver disease is the fifth most common cause of premature death in the Western world, with the irreversible damage caused by fibrosis, and ultimately cirrhosis, a primary driver of mortality. Early detection of fibrosis would facilitate treatment of the underlying liver disease to limit progression. Unfortunately, most cases of liver disease are diagnosed late, with current strategies reliant on invasive biopsy or fragile lab-based antibody technologies. A robust, fully synthetic fluorescent-polymer sensor array is reported, which, rapidly (in 45 minutes), detects liver fibrosis from low-volume serum samples with clinically relevant specificity and accuracy, using an easily readable diagnostic output. The simplicity, rapidity, and robustness of this method make it a promising platform for point-of-care diagnostics for detecting and monitoring liver disease.

Point of care (PoC) diagnostics based on blood serum allow rapid and accurate diagnosis of more disease states than any other body fluid, and can be administered at the hospital bedside, at local clinics, or in the patient's home.^[1–3] PoC diagnostics can greatly improve care in both urban and rural communities by enabling more frequent monitoring of patient health, yielding both lower costs and shorter analysis times.^[4] In all areas of biomedicine, continuous longitudinal collection of health-data can lower patient mortality rates by facilitating earlier intervention.^[5] Serum is however a challenging medium for sensors, containing thousands of different proteins, at concentrations ranging over ten orders of magnitude, as well as salts, carbohydrates, and lipids.^[6] Serum-based PoC diagnostics must be quick, robust, low-cost, and use small sample volumes of serum. Additionally, serum-based diagnostics must be

designed from materials that are resistant to fouling by protein adsorption and degradation by enzymes, yet can still operate with clinically relevant specificity and sensitivity.

Liver disease is a particularly significant yet underexplored target for PoC blood testing, despite its prevalence and socio-economic costs. In contrast to cancer and heart disease, mortality from liver disease has increased over the last 30 years and is now the fifth most common cause of middle-aged death in Western society. Liver disease costs health services tens of billions of dollars each year,^[7] and could affect an estimated 30% of people in the US.^[8]

Disease severity, prognosis, and response to treatment for liver disease are largely determined by the stage of liver fibrosis (scarring).^[9] Liver health is strongly manifested in blood composition,^[10,11] with immunosensing platforms such as the “enhanced liver fibrosis” test (ELF) used to assess and monitor fibrosis progression from serum without invasive biopsies currently in standard use.^[11,12] These blood tests quantify multiple serum biomarkers to provide a measure of liver fibrosis, shortening time to treatment, and improving assessment of patient prognosis.^[12,13] The instability of the bioconjugates used for biomarker detection, however, requires sending samples to centralized pathology laboratories for analysis, increasing cost and complexity of tests, and delaying diagnosis and treatment for patients.^[14,15]

Cross-reactive “chemical nose/tongue” sensing arrays have emerged as a strategy to rapidly profile complex chemical and

Dr. W. J. Peveler
Division of Biomedical Engineering
School of Engineering
College of Science and Engineering
University of Glasgow
Glasgow G12 8LT, UK

Dr. W. J. Peveler, Prof. C. J. Carmalt
Department of Chemistry
University College London
20 Gordon Street, London WC1H 0AJ, UK

 The ORCID identification number(s) for the author(s) of this article can be found under <https://doi.org/10.1002/adma.201800634>.

© 2018 The Authors. Published by WILEY-VCH Verlag GmbH & Co. KGaA, Weinheim. This is an open access article under the terms of the Creative Commons Attribution License, which permits use, distribution and reproduction in any medium, provided the original work is properly cited.

The copyright line for this article was changed on 2 August 2018 after original online publication.

DOI: 10.1002/adma.201800634

R. F. Landis, M. Yazdani, Prof. V. M. Rotello
Department of Chemistry
University of Massachusetts Amherst
710 North Pleasant Street, Amherst, MA 01003, USA
E-mail: rotello@chem.umass.edu

Dr. J. W. Day, Prof. W. M. Rosenberg
Institute for Liver & Digestive Health
University College London
Division of Medicine
Royal Free Hospital
Rowland Hill Street, London NW3 2PF, UK
E-mail: w.rosenberg@ucl.ac.uk

R. Modi, Prof. W. M. Rosenberg
iQur Ltd
LBIC
2 Royal College Street, London NW1 0NH, UK

biological systems using robust synthetic receptors.^[16,17] These array-based sensors generate patterns from the sample that are subsequently classified to generate algorithms for identifying analytes. Synthetic solution-based arrays have been successful in “fingerprinting” and distinguishing proteins spiked in serum,^[18] as well as in cell and cell lysate sensing.^[19–21] Pattern-based serum sensing, however, has not been widely demonstrated, with neither examples based on robust multiplexed (single well) sensing nor examples that can stage a disease.^[22–24] Such a “hypothesis-free” approach would allow for disease detection using multiple known and unknown biomarkers in a single assay.

We present here a robust, multiplexed fluorescent-polymer-based sensor platform that detects liver fibrosis from a small-volume serum sample, with clinically relevant accuracy. The sensor elements have been engineered to act both as cross-reactive recognition and transduction elements, with modulated fluorescence provided by simple chemical moieties. This chemical approach generates a modular and reproducible array design, simplifying implementation relative to most or multipart sensor systems.^[18,25] By mixing three of the chemically stable polymers in a single, multiplexed array, an information-rich output (four fluorescent channels) is generated from a single sample measurement (Figure 1). This array can accurately distinguish non-fibrotic patients from those with early stage liver fibrosis, in a cohort of 65 benchmarked patient samples. Significantly, the polymer sensor does not degrade in ambient conditions, dramatically increasing the viability of this platform for PoC diagnostics relative to the biologicals used in current methods.

Our sensor array is based on a poly(oxanorborneneimide) (PONI) random copolymer scaffold,^[26] chosen for its ease of modification and good compatibility with biological media.^[27] The polymer featured benzoate (Bz) monomers to provide protein recognition and reactive sites for dye attachment using NHS-ester chemistry, with the overall fluorophore loading controlled by proportionate mixing of the two monomer units in

the PONI backbone (Figure 1e). The number of repeat units (≈ 40) was kept low to enhance stability in serum. This scaffold was decorated with environmentally responsive fluorescent dyes that act both as cross-reactive recognition and transduction elements, providing a straightforward array design.

Three PONI-polymer sensor elements were synthesized bearing pendant pyrene (Py), dapoxyl (Dap), and PyMPO dyes (Figure 1e). Overall, the concise 3-polymer sensor generates four channels from a single sample measurement. Each polymer displayed a change in fluorescence intensity upon the addition of specific proteins to the polymer solution, due to changes in the ionic strength, pH, and supramolecular interactions of the dyes (Figure 1f).^[28,29] The Py polymer displays a principle emission at 380 nm and an excimer emission at 480 nm.^[30] The former band is ratiometrically sensitive to the polarity of the pyrene microenvironment, and the latter to the physical separation of multiple pyrenes.^[31] Dapoxyl and PyMPO gave emission in the yellow/orange region of the spectrum at 580 and 570 nm, respectively, but had well separated excitation bands (330 and 416 nm) providing spectral resolution in the mixed system (Figure S1, Supporting Information).

Initial experiments were performed by testing the array against 40 μL human serum samples, the amount available from a single drop finger-stick sample, and hence suitable for PoC applications.^[32] Increases in fluorescence intensity were observed for all polymers in differing ratios on mixing with serum. While some red- or blueshifting of the peaks were also seen, the intensity changes were the major factor (Figure S2, Supporting Information). In the first tests, the ability of the array to measure perturbations in protein levels in human serum was tested by spiking analyte proteins (human serum albumin (HSA), immunoglobulin G (IgG), transferrin (Trf), fibrinogen (Fib), and alpha-1-antitrypsin (a1AT)) into diluted or full human serum (Figures S3 and S4 and Table S1, Supporting Information). Full details are given in the Supporting Information.

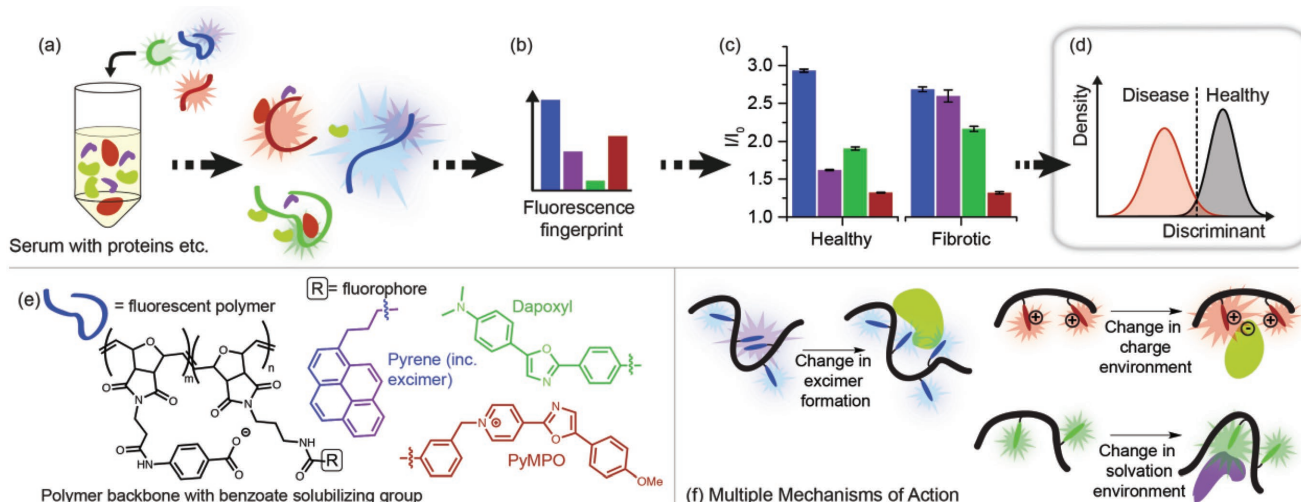


Figure 1. a) Generation of a fluorescent fingerprint through serum protein–polymer interactions, giving, b) a fluorescent fingerprint. c) Exemplar outputs for healthy and fibrotic patients used for, d) discriminant analysis for fibrosis detection. e) The molecular structures of the fluorescent polymers – $m:n \approx 9:1$. f) The interaction of the dyes and their environment leads to modulation of their fluorescence through changes in physical arrangement, solvation, and charge, with pyrene providing two fluorescence channels, one principal emission and one excimer emission.

Table 1. Values of HA, PIIINP, and TIMP-1 used to calculate the ELF score for each sample. The range and mean are given for the three fibrosis groups (healthy, mild-moderate, and severe) as determined on the basis of the ELF score.

Fibrosis Group	<i>n</i>	Range of value (mean)			
		HA [ng mL ⁻¹]	PIIINP [ng mL ⁻¹]	TIMP-1 [ng mL ⁻¹]	ELF Score
Healthy	16	4.72–17.62 (9.63)	2.32–9.51 (6.66)	147.0–235.3 (197.9)	7.03–7.94 (7.64)
Mild-mod	17	14.45–118.68 (56.82)	6.76–17.07 (10.35)	159.5–279.0 (230.9)	8.23–10.34 (9.39)
Severe	17	92.44–811.86 (367.83)	11.33–57.27 (22.46)	193.2–693.1 (347.5)	10.50–13.38 (11.69)

The array was then tested to determine whether it could “fingerprint” liver fibrosis in a serum sample, using the hypothesis-free approach to provide a potentially clinically relevant assay. The ELF test, based on three serum biomarkers hypothetically linked to liver fibrosis, was used as our benchmark, due to its use as a gold-standard for fibrosis detection in a wide range of liver diseases.^[11,33] Sixty-five human serum samples were previously quantified for hyaluronic acid (HA), PIIINP (N-terminal propeptide of Type III collagen), and TIMP-1 (a tissue inhibitor of metalloproteinase) with the commercial ELF test, to generate an ELF score for each sample (Table 1).

This sample library represented an “averaged” disease landscape, reflecting the spectrum of liver diseases encountered in hospital practice, across age and gender, with equal representation of healthy patients and patients with moderate and severe fibrosis. While age and gender can be used as a proxy for “risk factor,” they were not used here, nor in the ELF scoring of the samples.^[33] Fifty samples were categorized into three groups on the basis of their ELF score: healthy (ELF < 8.0), mild-moderate fibrosis (8.0 ≤ ELF < 10.5) or severe fibrosis (ELF ≥ 10.5), set as per National Institute for Health and Care Excellence (NICE) guidance for liver fibrosis.^[34] The second set of 15 samples was set aside as an independent validation set (Table S2, Supporting Information).

Serum was added to the polymer sensor solution in a standard microplate for fibrosis detection studies. Samples were measured in replicate and the ratiometric change in each fluorescent readout used to generate the fluorescent fingerprint of each sample (Figure S5 and Table S3, Supporting Information). Sensor response was generated in 30–45 min, much faster than current methods requiring multiple hours.

The fluorescent patterns generated from mixing the polymer and serum samples were processed with a simple LDA (linear discriminant analysis) model. Each polymer displays a change in fluorescence intensity upon the addition of serum containing various proteins to the polymer solution, due to changes in the ionic strength, pH, and supramolecular interactions of the dyes (Figure 1f). The relative change in the emission intensity (I/I_0) of each polymer is recorded for each sample in the “training” dataset (Figure 1c). The data processing with LDA takes the four recorded polymer emissions for each sample and creates a linear combination of the input data—a “score.” This is done in such a way as to minimize the variance between samples of the same group (e.g., all “healthy” samples have a similar score) while maximizing the difference between samples of different groups (scores for “healthy” and “fibrotic” samples are as different as possible) (Figure 1d). Alternative, nonlinear models such as quadratic discriminant analysis, or support vector machines were also tested, but had issues of overfitting the data in this case.

For the samples of unknown liver health in the “test” dataset, the four polymer emissions are recorded for each as before. These data were compared quantitatively to the training set through their Mahalanobis distance^[35] to the previously defined groups (e.g., healthy or fibrotic), a technique that provides effective classification of new samples.^[20,36]

A diagnostic test for healthy, mild-moderate or severe fibrosis was developed by training this model against the first 50 patient samples. This classification model can distinguish between the three individual groups with 60% accuracy (Figure 2a; Figure S6, Supporting Information), with the most misclassification occurring between mild-moderate and severe fibrosis. An independent reference sample set was analyzed with the same model ($n = 15$, across all classes), with LDA giving 66.7% accuracy using the same 3-group model (Table S6, Supporting Information).

Notably, the array could discriminate between healthy samples and those from patients with fibrosis, a critical distinction of interest to clinicians. Thus, further analysis was undertaken using the healthy group versus a total fibrotic group combining mild/moderate and severe into one class.

Multiple common liver biomarkers were measured in the samples and correlated to the classification accuracy (Figure S7, Supporting Information). Some small correlations between TIMP-1 levels and misclassification of the fibrotic samples were evident, but a lack of overall correlation between total protein concentrations or key proteins and the misclassified results indicate that there are indeed multiple biomarkers being analyzed to generate the result. Ultimately it is this signature that is determined and can be linked back to the disease; this is an area we are currently investigating further for future biomarker discovery and improvements to fibrosis detection.

Accuracy and sensitivity were determined through receiver operator characteristic (ROC) curve analysis (Figure 2b).^[37] Improvement in a classifier is indicated by an increase in the overall summary metric of area under ROC curve (AUROC), with the value ranging between 1 (perfect) and 0.5 (no better than chance), and the standard AUROC required of a diagnostic test for clinical relevancy is >0.80 (although other measures such as positive/negative predictive values must be considered too).^[38]

The LDA model was recalculated as described above to distinguish healthy patients from those with any degree of fibrosis (Figure 2c). This model classified the data with 80% accuracy and generated a single LDA score for each data point. In the 15-sample test set, the classification was also 80% for healthy samples versus fibrotic samples (Table S4, Supporting Information). The means of the two groups in the LDA were significantly different (t -test, $p < 0.001$) and the cut-off between healthy and fibrotic was determined to be an LDA score of 0.304 (Figure 2c). On this basis, sensitivity (the ratio of true

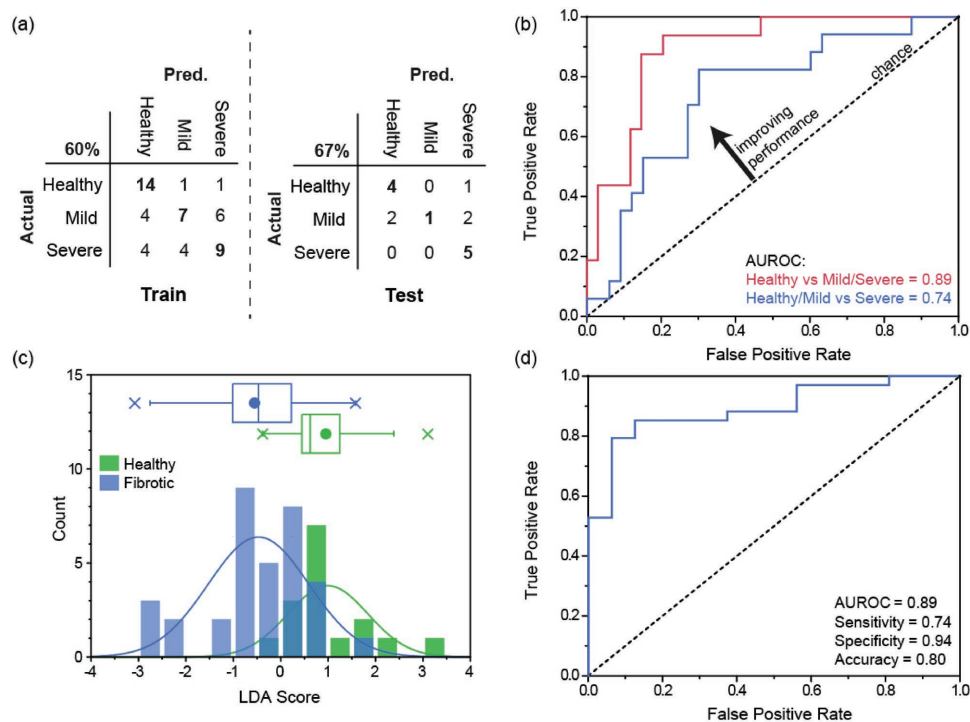


Figure 2. a) LDA models built on the training set for a 3-group model provides 60% accuracy as echoed in the test data. b) ROC analysis for this model showed that most misclassification arose between mild-moderate and severe fibrosis. c) LDA performed using two groups only—healthy versus all fibrosis. The box plot gives data max/min (x) and the tails are set at 1.5 times the interquartile range. The box gives the upper and lower quartiles, the median, and the mean (•). The histogram is marked with normal distributions fitted to the full data. d) ROC analysis of the two-group diagnostic study, with accuracy improved to 80% and an AUROC of 0.89.

positives to total positive values found) was calculated as 74% and specificity as 94% (the ratio of true negatives to total negative values found). The AUROC was found to be 0.89 (Figure 2d), greater than the threshold for clinical relevance. Our new polymer-based test is fully comparable to other methods of diagnosing and staging fibrosis, such as elastography (AUROC = 0.84–0.89)^[39] and other serum biomarker tests (AUROC = 0.76–0.89).^[33,40] Therefore the result represents a substantial advance in both the use of array-based sensors for disease diagnosis, and in the detection of fibrosis, and a next step will be to recruit a larger cohort for better assessment of clinical utility.

In summary, we have fabricated a new multiplexed fluorescent-polymer sensor array capable of detecting liver fibrosis using low volume serum. The accuracy and sensitivity of our hypothesis-free platform compares favorably against other leading biomarker-driven methods for detecting fibrosis, but does not require the specialist instrumentation of, for example, elastography, while the robustness of the polymer platform is unprecedented for serum assay liver diagnostics, removing the need for cold-chain transport and storage. This combination of excellent accuracy, fast result time, and stability provides a promising avenue for translation into a rapid, robust, point-of-care disease diagnostic for near-patient testing at home or in a primary care setting.

Experimental Section

Polymer Synthesis: Monomers and polymers were synthesized as described in the Supporting Information and previous publication.^[41]

ELF Characterization: Serum samples were anonymous, unlinked, residual samples discarded after clinical evaluation from the liver clinics at the Royal Free Hospital, London, of volume between 0.5 and 1 mL and stored at $-80\text{ }^{\circ}\text{C}$. The samples represented a range of etiologies of liver disease and were from a range of ages and genders. Serum had been previously collected and analyzed using standard iQur protocols, as detailed in the Supporting Information. All samples were collected, stored, and analyzed in compliance with Protocol IRAS: 197224, which has undergone ethical review and was approved by the London-South East Research Ethics Committee on behalf of the UK National Research Ethics Committee.

Array Methodology: The polymers were diluted and mixed in phosphate buffered saline (PBS), pH 7.4 $150 \times 10^{-3}\text{ M}$ to final concentrations of $4.7 \times 10^{-6}\text{ M}$ for PONI-Bz-Py, $13.3 \times 10^{-6}\text{ M}$ for PONI-Bz-Dap, and $6.0 \times 10^{-6}\text{ M}$ for PONI-Bx-PyMPO. For the spiked serum experiments 190 μL of polymer solution was loaded into a 96-well plate, and 10 μL of serum was added. For the fibrosis sensing, it was determined that larger fluorescence changes could be achieved with a slightly larger volume of serum. Therefore, future experiments used 40 μL of serum to maximize I/I_0 while maintaining a reasonable dynamic range: 160 μL of the resultant polymer solution was loaded into a 96-well plate following the injection of the specimen (40 μL of patient serum specimens). As a control experiment, PBS solution was injected instead of the serum specimens to account for dilution (I_0). The samples were incubated for 45 min, with measures made at 0, 15, 30, and 45 min. The emission spectra of the polymers were recorded at the optimal excitation/emission (Ex/Em) wavelengths: PONI-Bz-Py with Ex/Em 346/380 nm and an excimer emission 346/480 nm. PONI-Bz-Dap with Ex/Em 330/580 nm. PONI-Bz-PyMPO with Ex/Em 416/570 nm, using a fluorescence microplate reader, from each well plate (I) and is normalized against the PBS reference; I/I_0 .

Three to six replicates were obtained for each specimen, dependant on residual volume, and the 45 min data were used and averaged.

Standard deviations of the averages (the coefficient of variation) were 8% or less. Fifty patient training set samples and four channels from the change in the major excitation-emission of the three PONI-Bz polymers generated a 50×4 data matrix. LDA was applied using SYSTAT and JMP software packages. The canonical scores generated by the LDA model were used to classify the training samples and a separate test set of 15 samples; five each of healthy, mild, and severe. In the case of healthy versus fibrotic classification, a single canonical score was generated and significance of difference between the two groups tested with a two-group *t*-test. ROC analysis performed in Origin Pro generated a ROC curve and AUROC statistics.

Supporting Information

Supporting Information is available from the Wiley Online Library or from the author.

Acknowledgements

W.J.P. and R.F.L. contributed equally to this work. W.J.P. was supported by a Royal Society International Exchange Grant, and thanks the EPSRC for a Doctoral Prize Fellowship (EP/M506448/1) and the University of Glasgow for an LKAS Fellowship. W.M.R. is an NIHR Senior Investigator and acknowledges the UCLH NIHR Biomedical Research Centre for funding. V.M.R. acknowledges the NIH (GM077173). Prof. Sandy Macrobert is thanked for access to plate reading instrumentation.

Conflict of Interest

W.M.R. received a speaker bureau from Siemens Healthineers and is a stockholder in iQur Ltd., inventors of the ELF test. R.M. is an employee of iQur Ltd.

Keywords

arrays, fluorescent polymers, liver fibrosis, multichannels, point of care

Received: January 29, 2018

Revised: March 19, 2018

Published online: May 24, 2018

- [1] E. Petryayeva, W. R. Algar, *RSC Adv.* **2015**, *5*, 22256.
- [2] N. R. Pollock, J. P. Rolland, S. Kumar, P. D. Beattie, S. Jain, F. Noubary, V. L. Wong, R. A. Pohlmann, U. S. Ryan, G. M. Whitesides, *Sci. Transl. Med.* **2012**, *4*, 152ra129.
- [3] G. Xu, D. Nolder, J. Reboud, M. C. Oguike, D. A. van Schalkwyk, C. J. Sutherland, J. M. Cooper, *Angew. Chem., Int. Ed.* **2016**, *55*, 15250.
- [4] N. Bilbey, S. Lalani, *UBCMJ* **2011**, *2*, 7.
- [5] V. Gubala, L. F. Harris, A. J. Ricco, M. X. Tan, D. E. Williams, *Anal. Chem.* **2012**, *84*, 487.
- [6] R. Pieper, C. L. Gatlin, A. J. Makusky, P. S. Russo, C. R. Schatz, S. S. Miller, Q. Su, A. M. McGrath, M. A. Estock, P. P. Parmar, M. Zhao, S.-T. Huang, J. Zhou, F. Wang, R. Esquer-Blasco, N. L. Anderson, J. Taylor, S. Steiner, *Proteomics* **2003**, *3*, 1345.
- [7] R. Williams, R. Aspinall, M. Bellis, G. Camps-Walsh, M. Cramp, A. Dhawan, J. Ferguson, D. Forton, G. Foster, S. I. Gilmore, M. Hickman, M. Hudson, D. Kelly, A. Langford, M. Lombard, L. Longworth, N. Martin, K. Moriarty, P. Newsome, J. O'Grady, R. Pryke, H. Rutter, S. Ryder, N. Sheron, T. Smith, *Lancet* **2014**, *384*, 1953.
- [8] M. H. Le, P. Devaki, N. B. Ha, D. W. Jun, H. S. Te, R. C. Cheung, M. H. Nguyen, *PLoS One* **2017**, *12*, e0173499.
- [9] J. Rehm, A. V. Samokhvalov, K. D. Shield, *J. Hepatol.* **2013**, *59*, 160.
- [10] N. H. Afdhal, D. Nunes, *Am. J. Gastroenterol.* **2004**, *99*, 1160.
- [11] W. M. C. Rosenberg, M. Voelker, R. Thiel, M. Becka, A. Burt, D. Schuppan, S. Hubscher, T. Roskams, M. Pinzani, M. J. P. Arthur, *Gastroenterology* **2004**, *127*, 1704.
- [12] Q. Xie, X. Zhou, P. Huang, J. Wei, W. Wang, S. Zheng, *PLoS One* **2014**, *9*, e92772.
- [13] J. Parkes, P. Roderick, S. Harris, C. Day, D. Mutimer, J. Collier, M. Lombard, G. Alexander, J. Ramage, G. Dusheiko, M. Wheatley, C. Gough, A. Burt, W. M. C. Rosenberg, *Gut* **2010**, *59*, 1245.
- [14] W. J. Peveler, M. Yazdani, V. M. Rotello, *ACS Sensors* **2016**, *1*, 1282.
- [15] J. Bordeaux, A. Welsh, S. Agarwal, E. Killiam, M. Baquero, J. Hanna, V. Anagnostou, D. Rimm, *Biotechniques* **2010**, *48*, 197.
- [16] W. J. Peveler, W. R. Algar, *ACS Chem. Biol.* **2018**, <https://doi.org/10.1021/acscchembio.7b01022>.
- [17] L. Guerrini, E. Garcia-Rico, N. Pazos-Perez, R. A. Alvarez-Puebla, *ACS Nano* **2017**, *11*, 5217.
- [18] M. De, S. Rana, H. Akpinar, O. R. Miranda, R. R. Arvizo, U. H. F. Bunz, V. M. Rotello, *Nat. Chem.* **2009**, *1*, 461.
- [19] A. Bajaj, O. R. Miranda, I. B. Kim, R. L. Phillips, D. J. Jerry, U. H. F. Bunz, V. M. Rotello, *Proc. Natl. Acad. Sci. USA* **2009**, *106*, 10912.
- [20] S. Rana, N. D. B. Le, R. Mout, K. Saha, G. Y. Tonga, R. E. S. Bain, O. R. Miranda, C. M. Rotello, V. M. Rotello, *Nat. Nanotechnol.* **2015**, *10*, 65.
- [21] N. D. B. Le, G. Yesilbag Tonga, R. Mout, S. T. Kim, M. E. Wille, S. Rana, K. A. Dunphy, D. J. Jerry, M. Yazdani, R. Ramanathan, C. M. Rotello, V. M. Rotello, *J. Am. Chem. Soc.* **2017**, *139*, 8008.
- [22] Y. Chen, Y. Zhang, F. Pan, J. Liu, K. Wang, C. Zhang, S. Cheng, L. Lu, W. Zhang, Z. Zhang, X. Zhi, Q. Zhang, G. Alfranca, J. M. de la Fuente, D. Chen, D. Cui, *ACS Nano* **2016**, *10*, 8169.
- [23] M. K. Nakhleh, H. Amal, R. Jeries, Y. Y. Broza, M. Aboud, A. Gharra, H. Ivgi, S. Khatib, S. Badarneh, L. Har-Shai, L. Glass-Marmor, I. Lejbkovicz, A. Miller, S. Badarny, R. Winer, J. Finberg, S. Cohen-Kaminsky, F. Perros, D. Montani, B. Girerd, G. Garcia, G. Simonneau, F. Nakhoul, S. Baram, R. Salim, M. Hakim, M. Gruber, O. Ronen, T. Marshak, I. Doweck, O. Nativ, Z. Bahouth, D.-Y. Shi, W. Zhang, Q.-L. Hua, Y.-Y. Pan, L. Tao, H. Liu, A. Karban, E. Koifman, T. Rainis, R. Skapars, A. Sivins, G. Ancans, I. Liepniece-Karele, I. Kikuste, I. Lasina, I. Tolmanis, D. Johnson, S. Z. Millstone, J. Fulton, J. W. Wells, L. H. Wilf, M. Humbert, M. Leja, N. Peled, H. Haick, *ACS Nano* **2017**, *11*, 112.
- [24] S. Xu, Y. Wu, X. Sun, Z. Wang, X. Luo, *J. Mater. Chem. B* **2017**, *5*, 4207.
- [25] J. Han, B. Wang, M. Bender, J. Pfisterer, W. Huang, K. Seehafer, M. Yazdani, V. M. Rotello, C. M. Rotello, U. H. F. Bunz, *Polym. Chem.* **2017**, *8*, 2723.
- [26] Z. M. Al-Badri, G. N. Tew, *Macromolecules* **2008**, *41*, 4173.
- [27] T. M. Reineke, *ACS Macro Lett.* **2016**, *5*, 14.
- [28] J. Min, J. W. Lee, Y.-H. Ahn, Y.-T. Chang, *J. Comb. Chem.* **2007**, *9*, 1079.
- [29] S. Charier, O. Ruel, J. B. Baudin, D. Alcor, J. F. Allemand, A. Meglio, L. Jullien, B. Valeur, *Chem. - Eur. J.* **2006**, *12*, 1097.
- [30] G. Bains, A. B. Patel, V. Narayanaswami, *Molecules* **2011**, *16*, 7909.
- [31] G. K. Bains, S. H. Kim, E. J. Sorin, V. Narayanaswami, *Biochemistry* **2012**, *51*, 6207.
- [32] L. Dalton, *ACS Cent. Sci.* **2016**, *2*, 878.
- [33] European Association for Study of Liver, Asociacion Latinoamericana para el Estudio del Hígado, *J. Hepatol.* **2015**, *63*, 237.

- [34] National Institute for Health and Care Excellence, *Non-Alcoholic Fatty Liver Disease (NAFLD): Assessment and Management (NICE Guideline NG49)* **2016**.
- [35] R. G. Brereton, *Chemometrics*, John Wiley & Sons, Ltd, Chichester, UK **2003**.
- [36] W. J. Peveler, A. Roldan, N. Hollingsworth, M. J. Porter, I. P. Parkin, *ACS Nano* **2016**, *10*, 1139.
- [37] M. H. Zweig, G. Campbell, *Clin. Chem.* **1993**, *39*, 561.
- [38] J. Fan, S. Upadhye, A. Worster, *Can. J. Emerg. Med.* **2006**, *8*, 19.
- [39] A. Baranova, P. Lal, A. Biredinc, Z. M. Younossi, *BMC Gastroenterol.* **2011**, *11*, 91.
- [40] Y. Lurie, M. Webb, R. Cytter-Kuint, S. Shteingart, G. Z. Lederkremer, *World J. Gastroenterol.* **2015**, *21*, 11567.
- [41] R. F. Landis, A. Gupta, Y.-W. Lee, L.-S. Wang, B. Golba, B. Couillaud, R. Ridolfo, R. Das, V. M. Rotello, *ACS Nano* **2017**, *11*, 946.